

Fabrication of cross-ply C_f/C -SiC composites and the investigation of pyrolysis conditions on their properties

Kati Raju, Seyoung Kim*, Young-Hoon Seong, Soo-Hyun Kim and In-Sub Han

Energy Efficiency and Materials Research Division, Korea Institute of Energy Research, Daejeon 34129, Korea

The fabrication of continuous carbon fiber-reinforced carbon-silicon carbide matrix (C_f/C -SiC) cross-ply composites is highly attractive from a practical viewpoint due to their homogeneous microstructures and isotropic mechanical properties. However, the properties of C_f/C -SiC composites depend significantly on their processing conditions and temperatures, especially the pyrolysis conditions and temperatures. In this study, cross-ply C_f/C -SiC composites were fabricated using different pyrolysis protocols with phenolic resin via a liquid silicon infiltration. The effects of the pyrolysis conditions on the microstructures of the composites and their mechanical properties as well as on crack formations were evaluated at room temperature. Pyrolysis was performed at 600 °C for 1 h in a nitrogen atmosphere at different heating rates. The flexural strength varied from a minimum of 47 ± 3 MPa to a maximum of 62 ± 6 MPa (~35% increase) depending on the pyrolysis conditions.

Keywords: Pyrolysis; Microstructure; C_f/C -SiC composites; Flexural strength.

Introduction

Research into the fabrication of continuous carbon fiber-reinforced carbon-silicon carbide matrix composites (C_f/C -SiC) is active at present because of their remarkable properties, such as low density, low coefficient of thermal expansion, high fracture toughness, high specific stiffness, and excellent oxidation resistance [1-4]. Due to these outstanding properties, these composites are recognized as potential candidates for applications in many advanced technological industries, including the automotive, energy, aerospace, and defense sectors [2-8]. The global market for these composites is increasing rapidly and it was reported that in the aerospace sector alone, they will be worth an estimated value of ~1.07 trillion US\$ by 2028 because of the manufacture of about 231,000 new aircraft engines [9].

Various fabrication techniques have been developed for manufacturing C_f/C -SiC composites, including liquid silicon infiltration (LSI), chemical vapor infiltration (CVI), and polymer impregnation and pyrolysis (PIP) [1, 10-12]; each of these techniques has certain advantages and disadvantages. In particular, the CVI and PIP methods employ many hazardous and cost-ineffective reactive gases and liquid precursors, respectively; these processes are very time consuming (> 24 h). Moreover, the fabrication of complex and large-sized composites is very difficult. From an industrial viewpoint, it has been demonstrated that LSI is an effective and economically

viable technique for fabricating C_f/C -SiC composites [1, 2]. Its advantages mainly include low costs, short fabrication periods (~3 h), low residual porosities, and the simplicity of large, complex, and near-net shaping. However, disadvantages such as the presence of residual silicon and fiber damage due to the exothermic reaction of silicon with carbon limit the usage of LSI. Nonetheless, these problems can be overcome by adjusting the processing parameters and coating with a suitable interphase layer wherever required.

Curing, pyrolysis, carbonization, and siliconization are the main sequential steps involved in the fabrication of C_f/C -SiC composites via LSI. Fig. 1 presents flow-chart for a typical LSI technique. Carbonization at higher temperatures may be applied sometimes after pyrolysis depending on the requirements. After preparing a carbon fiber-reinforced plastic (CFRP) with the desirable preform and polymer, curing is normally performed at lower temperatures (< 250 °C), where cross-linking of the polymer occurs and it hardens. Different thermosetting and thermoplastic polymers can be used, such as polyetheretherketone, polyetherimide, phenolic, silicone, and epoxy resins [13-16]. In the next step, pyrolysis is performed at moderate temperatures below 1,000 °C and the polymer is converted into amorphous/glassy carbon. Cracks are generated within the CFRP during pyrolysis due to shrinkage of the matrix. Subsequently, carbonization is conducted at temperatures greater than 1,600 °C in order to obtain the porous C_f/C preform. Finally, siliconization is performed at temperatures higher than 1,420 °C (melting temperature of Si), where the liquid silicon infiltrates under the driving capillary force and expands to fill the pores. Moreover, the

*Corresponding author:
Tel : +82-428603471
Fax: +82-428603133
E-mail: saykim@kier.re.kr

liquid silicon reacts with carbon in the porous preform to yield a dense $C_f/C-SiC$ composite.

Each step in the LSI process plays a crucial role in determining the final characteristics of the $C_f/C-SiC$ composites because their properties depend significantly on the processing conditions [16-18]. The pyrolysis of CFRP is considered a vital step because segment cracks (transverse), micro-cracks, and micro-delaminations start generating during this stage [19, 20]. The properties of composites are governed primarily by these crack patterns. However, these cracks can be controlled by adjusting parameters such as the pyrolysis temperature, heating rate, and fiber treatment, and by adding filler materials to the polymers [21-26]. Furthermore, the properties of $C_f/C-SiC$ composites depend greatly on the fibers employed, fiber orientation, fiber architecture, interphase coating layers, matrix phase, and many other factors [1, 27]. From a practical viewpoint, using cross-ply $C_f/C-SiC$ composites with homogeneous microstructures and isotropic mechanical properties is more attractive than employing woven and unidirectional composites. Cross-ply composites have received little attention in previous studies. Thus, in the present study, cross-ply $C_f/C-SiC$ composites were fabricated with different pyrolysis protocols via the LSI method. The microstructures of the composites and their mechanical

properties, such as the flexural strength and fracture toughness, were evaluated at room temperature.

Fabrication and Characterization

In order to fabricate cross-ply $C_f/C-SiC$ composites, unidirectional carbon fibers (T-300, Toray, Japan) of $6 \times 6 \text{ cm}^2$ in size were initially impregnated using phenolic resin (KRD-HM2, Kolon Chemical Co. Ltd, Korea). The volume fraction of fiber content was about 0.49%. CFRP was prepared by stacking 16-ply fabrics in alternative 0° and 90° directions under vacuum bagging, before slowly curing at 120°C for 24 h. The cured CFRP was heat-treated to achieve pyrolysis in a nitrogen atmosphere at 600°C for 1 h with two different temperature ramp-up rates of 25 and 50°C/h . The temperature was selected based on thermogravimetric analyses of phenolic resins in our previous studies and other reported data [24, 25, 28]. The carbonization of CFRP was performed at $1,600^\circ\text{C}$. LSI was conducted with the porous C_f/C preform at $1,600^\circ\text{C}$ in vacuum for 30 min. Four different composites were fabricated using different pyrolysis conditions as shown in Table 1 along with their labels.

The densities of the composites after LSI were experimentally determined using the well-known Archimedes' method [29]. The microstructures of the composites after pyrolysis and LSI were observed by scanning electron microscopy (SEM; Model: S-4800, Hitachi Co.). The flexural strengths of the composites were measured using the three-point bending test according to the ASTM C1161 standard with a universal testing machine (UTM: H5KT, Tinius Olsen, USA). Flexural

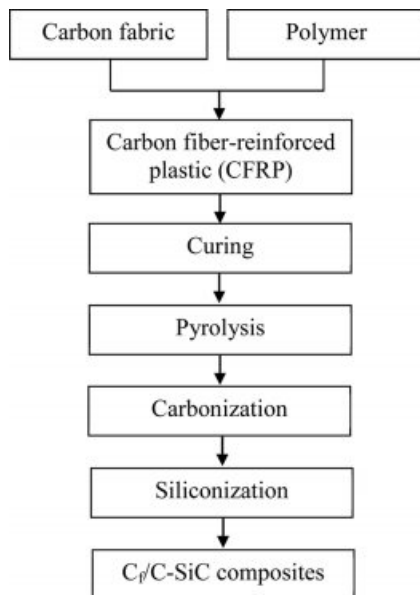


Fig. 1. Flow-chart for the fabrication of $C_f/C-SiC$ composites through LSI.

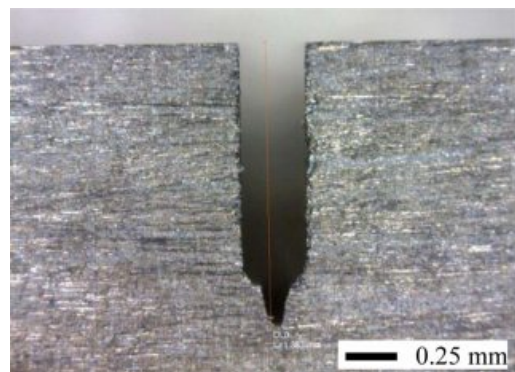


Fig. 2. SEVNB optical microscopic image of composite C4 used for fracture toughness test.

Table 1. Density, porosity, flexural strength and fracture toughness values for all of the composites.

Sample code	Pyrolysis temperature profile	Density (g/cc)	Porosity (%)	Flexural strength (MPa)	Fracture toughness ($\text{MPa}\cdot\text{m}^{1/2}$)
C1	$0 \sim 600^\circ\text{C}$ (50°C/h)	2.18 ± 0.04	1.15 ± 0.25	47 ± 3	1.76 ± 0.15
C2	$0 \sim 350^\circ\text{C}$ (50°C/h); $350 \sim 600^\circ\text{C}$ (25°C/h)	2.21 ± 0.02	0.37 ± 0.11	55 ± 7	1.79 ± 0.11
C3	$0 \sim 350^\circ\text{C}$ (25°C/h); $350 \sim 600^\circ\text{C}$ (50°C/h)	2.21 ± 0.01	0.52 ± 0.29	56 ± 4	1.81 ± 0.12
C4	$0 \sim 600^\circ\text{C}$ (25°C/h)	2.20 ± 0.07	0.44 ± 0.25	62 ± 6	1.88 ± 0.23

tests were conducted with a cross-head speed of 0.5 mm/s at room temperature using polished specimens with dimensions of $40^l \times 4^w \times 3^t$ mm³. The bending strengths were calculated based on the maximum load after fracture. The fracture toughness (K_{Ic}) of each composite was evaluated using the single edge V-notched beam method according to the ASTM C1421 standard. Fig. 2 shows optical microscopic image of a typical composite used for fracture toughness measurement. Averages based on five measurements were determined for the flexural strength and fracture toughness.

Results and Discussion

Previous studies have demonstrated the importance

of the pyrolysis conditions for the fabrication of composites via LSI [16, 30]. Chang et al. [16] studied the effects of the pyrolysis heating rate on the mechanical properties. They observed that the flexural strength decreased as the heating rate increased. This was attributed to the higher number of voids and cracks generated within the composite at higher heating rates. During pyrolysis, the phenolic resin was converted to amorphous/glassy carbon. The weight loss was substantial between temperatures of 400 ~ 700 °C (approximately 27.1%), which corresponded to more than 90% of the total gases that evolved [28]. Based on our previous thermogravimetric analyses of phenolic resins [24, 25], pyrolysis was performed at 600 °C in this study with heating rates of 25 and 50 °C/h. Fig. 3 shows SEM

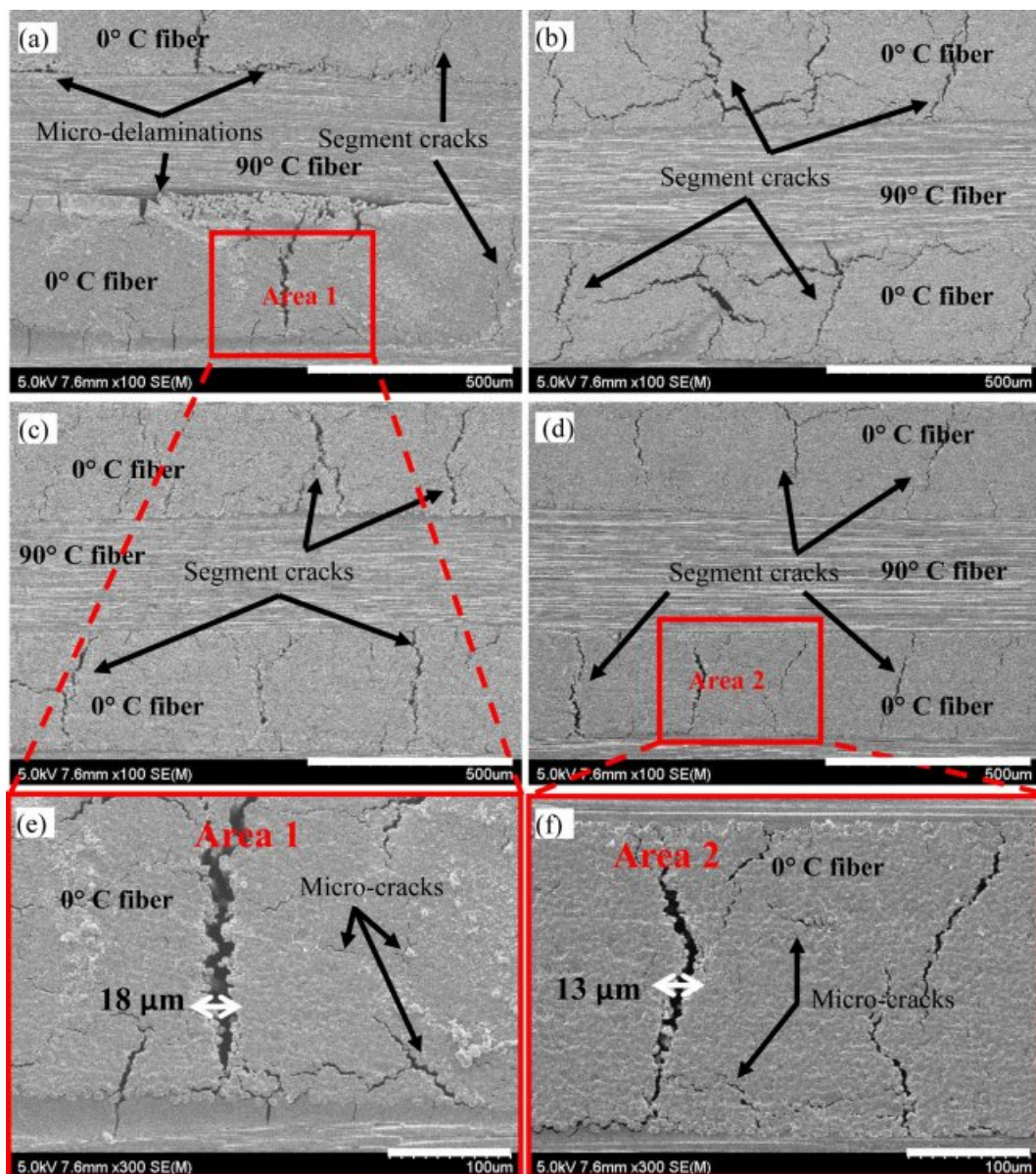


Fig. 3. (a-d) SEM images of all the composites after pyrolysis at 600 °C; magnified images of areas 1 and 2 in Figs. 3 (a) and (d) are shown in Figs. 3 (e) and (f), respectively.

images of all the composites after pyrolysis at 600 °C using different protocols. Magnified images of areas 1 and 2 in Figs. 3(a) and (d) are shown in Figs. 3(e) and (f), respectively. All the composites exhibited similar segment cracks and micro-cracks. However, sample C1 contained a few additional micro-delaminations, as shown in Fig. 3(a), which may be attributed to the higher heating rate of 50 °C/h. During the pyrolysis process, CFRP was transformed into a porous C_f/C structure via the development of cracks that allowed the liquid silicon to penetrate. Different cracks such as segment cracks (transverse) developed within the 0° fiber bundles and micro-delaminations in the opposite fiber bundles (0° and 90° directions). Moreover, some micro-cracks and voids also developed within the segments [23]. Each of these different types of cracks was generated due to an offset of the compressional stresses generated within the segments after the carbon matrix shrinks. The widths of the segment cracks were directly related to the pyrolysis temperature and heating rates. The widths of the segments were expected to increase as the temperature and heating rate increased. We found that when the heating rate decreased from 50 to 25 °C/h, the crack width also decreased from about 18 to 13 μm, as shown in Fig. 3(e & f). Table 1 presents the density and porosity values for all the four composites prepared using different pyrolysis conditions. Evidently, the density and porosity values were similar and they were not affected considerably by the pyrolysis

conditions.

SEM images of all the composites after LSI are compared in Fig. 4 at the same magnification (×100). The composites comprised carbon fibers in both the 0° and 90° directions, where the matrix consisted of carbon, residual silicon, and reacted SiC, and transverse cracks were present (within 0° C fiber). The cracks are marked by black arrows in Fig. 4, which clearly shows that all of the composites had similar microstructures. Higher magnification (×1,000) SEM micrographs of the entire composites are also compared in Fig. 5, which demonstrate that all of the samples exhibited similar fiber damage after LSI. These microstructures are comparable with those obtained in previous studies of C_f/C-SiC composites fabricated via LSI [30-34]. The cracks (transverse) occurred during cooling from higher temperatures after LSI because of the mismatched thermal expansion coefficients for C, Si, and SiC resulting in thermal residual stresses, as shown in Fig. 4. Figs. 4 and 5 indicate that all of the composites were fully infiltrated with molten silicon. Evidently, the carbon fibers were damaged and not fully protected as the silicon reached the carbon fibers surrounded by the carbon matrix and reacted to form SiC, possibly because temperatures higher than 2,000 °C are expected to allow the reaction between carbon and silicon to occur instantaneously [35]. In addition, the continuous formation of SiC was controlled by the diffusion of silicon through the previously formed SiC layer.

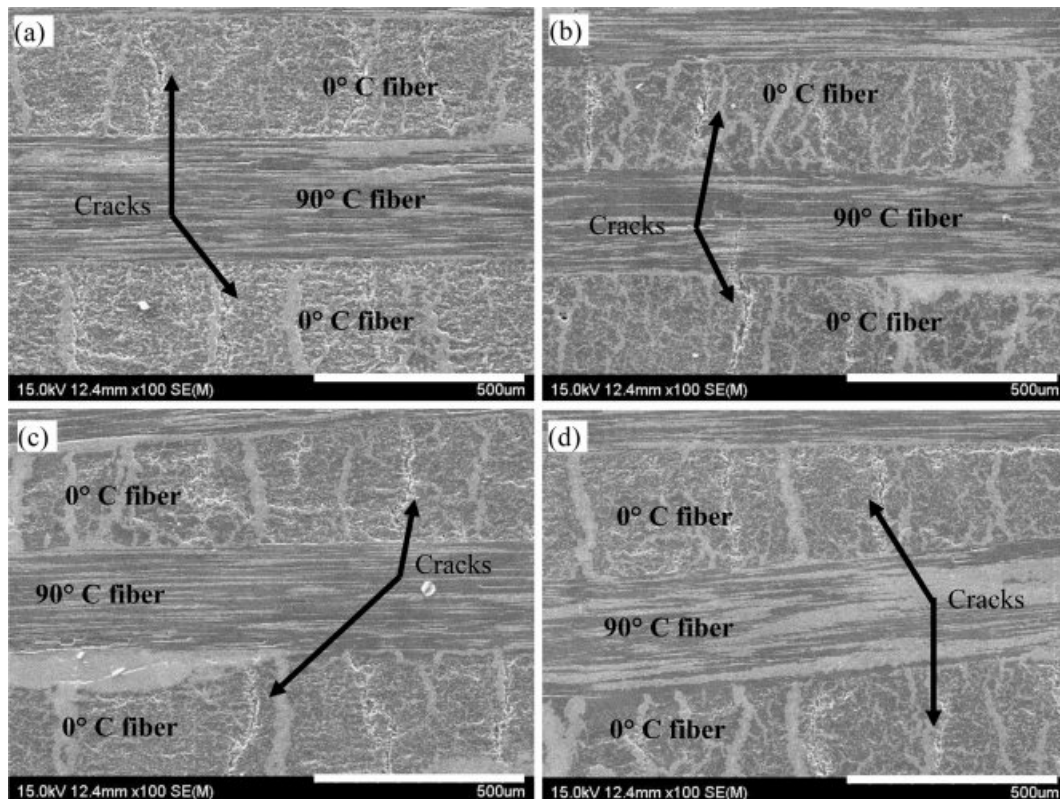


Fig. 4. SEM images of all the composites after LSI.

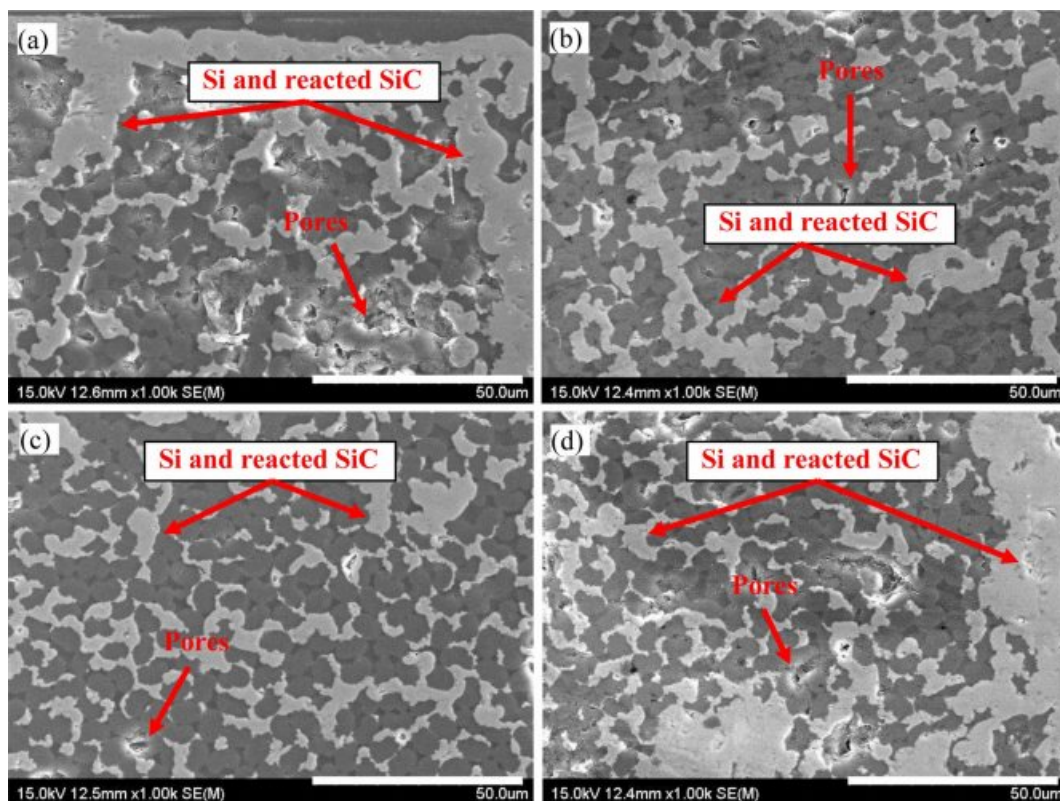


Fig. 5. Higher magnification ($\times 1,000$) SEM images of all the composites after LSI.

The flexural strength and fracture toughness values for all of the composites prepared under different pyrolysis conditions are compared in Table 1. The flexural strength varied from a minimum of 47 ± 3 MPa to a maximum of 62 ± 6 MPa ($\sim 35\%$ increase), and the fracture toughness varied from 1.76 to 1.88 $\text{MPa}\cdot\text{m}^{1/2}$ ($\sim 7\%$ increase), depending on the pyrolysis conditions. Among all of the composites, composite C4 had the greatest mechanical properties, with a flexural strength of 62 ± 6 MPa and fracture toughness of 1.88 $\text{MPa}\cdot\text{m}^{1/2}$. These mechanical properties were greatly improved compared with those of the other composites. Therefore, it can be concluded that C_f/C-SiC composites with superior mechanical properties were obtained using a typical heating rate of 25 °C/h. All of the composites exhibited brittle behavior and no fiber pull-out was observed after the mechanical tests, thereby indicating that all of the composites were characterized by strong interface bonding between the fiber and the matrix.

Therefore, considering the similar densities, porosities, and microstructures, and the availability of the same amount of carbon to react with silicon, except in the presence of some micro-delaminations (C1 composite), the mechanical properties decreased as the heating rate increased because more silicon reacted with carbon, and thus more fiber damage occurred, although the formation of SiC could enhance the mechanical properties.

Summary

In this study, cross-ply C_f/C-SiC composites were successfully fabricated using the LSI technique. We examined the effects of different pyrolysis conditions on crack formation as well as the microstructures and mechanical properties of the C_f/C-SiC composites. Pyrolysis of CFRP was performed at 600 °C for 1 h in a nitrogen atmosphere at two different heating rates of 25 and 50 °C/h before siliconization. The composites pyrolyzed at a heating rate of 25 °C/h exhibited superior mechanical properties. These results demonstrate that crack formation and the microstructures of composites can be modified by selecting suitable pyrolysis conditions. This is done in order to improve the mechanical properties of the microstructures.

Acknowledgement

The authors acknowledge financial support from the Korea Institute of Energy Research (KIER) under grant number B9-2433.

References

1. B. Heidenreich, *Ceramic Matrix Composites: Materials, Modeling and Technology* (Eds: N. P. Bansal, J. Lamon), John Wiley & Sons, Inc., Hoboken, US 2015, pp. 147-235.
2. W. Krenkel, B. Heidenreich, and R. Renz, *Adv. Eng. Mater.*

- 4 (2002) 427-436.
3. F. Christin, *Adv. Eng. Mater.* 4 (2002) 903-912.
4. H. A. El-Hija, W. Krenkel, and S. Hugel, *Int. J. Appl. Ceram. Technol.* 2 (2005) 105-113.
5. S. Schimdt, S. Beyer, H. Immich, H. Knabe, R. Meistring, and A. Gessler, *Int. J. Appl. Ceram. Technol.* 2 (2005) 85-96.
6. W. Krenkel and F. Berndt, *Mat. Sci. Eng. A* 412 (2005) 177-181.
7. J. Schmidt, M. Scheifflele, M. Crippa, F. Peterson, E. Urquiza, K. Sridharan, L. C. Olson, M. H. Anderson, T. R. Allen, and Y. Chen, *Int. J. Appl. Ceram. Technol.* 8 (2011) 1073-1086.
8. F. Infed, K. Handrick, H. Lange, A. Steinacher, S. Weiland, and C. Wegmann, *Acta Astronaut.* 70 (2012) 122-138.
9. N.P. Padture, *Nat. Mater.* 15 (2016) 804-809.
10. S. Dong, H. Wen, Q. Zhou, and Y. Ding, *J. Ceram. Process. Res.* 10 (2009) 278-285.
11. X. Peng, L. Zhuan, Z. Zi-bing, and X. Xiang, *J. Ceram. Process. Res.* 11 (2010) 335-340.
12. Q. Zhang, L. Cheng, L. Zhang, and N. Dong, *J. Ceram. Process. Res.* 14 (2013) 247-250.
13. T.-H. Ko, *Polym. Composite.* 14 (1993) 247-256.
14. J.-Y. Liu, K. Jian, Z.-H. Chen, Q.-S. Ma, and S. Wang, *Key Eng. Mater.* 368-372 (2008) 1022-1024.
15. F. Reichert, N. Langhof, and W. Krenkel, *Mater. Sci. Forum* 825-826 (2015) 232-239.
16. W.-C. Chang, C.-C. Ma, N.-H. Tai, and C.-B. Chen, *J. Mater. Sci.* 29 (1994) 5859-5867.
17. J. Chlopek and S. Blzewicz, *Carbon* 29 (1991) 127-131.
18. C.R. Choe, K. H. Lee, and B.I. Yoon, *Carbon* 30 (1992) 247-249.
19. J. Schulte-Fischedick, S. Seiz, N. Lutzenburger, A. Wanner, and H. Voggenreiter, *Composites: Part A* 38 (2007) 2171-2181.
20. J. Schulte-Fischedick, A. Zern, J. Mayer, M. Ruhle, and H. Voggenreiter, *Composites: Part A* 38 (2007) 2237-2244.
21. J. Jortner, *Carbon* 24 (1986) 603-613.
22. T.-H. Ko and P.-C. Chen, *J. Mater. Sci. Lett.* 10 (1991) 301-303.
23. F. Gao, J. W. Patrick, and A. Walker, *Carbon* 31 (1993) 103-108.
24. S. Kim, S.-K. Woo, I.-S. Han, D.-W. Seo, B.-K. Jang, and Y. Sakka, *J. Ceram. Soc. Jpn.* 118 (2010) 1075-4078.
25. J.H. Choi, S. Kim, S.-H. Kim, I.-S. Han, Y.-H. Seong, and H.J. Bang, *J. Ceram. Process. Res.* 20 (2019) 48-53.
26. Y. Cai, L. Cheng, H. Zhang, X. Yin, H. Yin, and G. Yan, *J. Alloy. Compd.* 770 (2019) 989-994.
27. W.-S. Kuo and T.-W. Chou, *J. Am. Ceram. Soc.* 78 (1995) 745-755.
28. T.-H. Ko, W.-S. Kuo, and Y.-H. Chang, *J. Appl. Polym. Sci.* 81 (2001) 1084-1089.
29. ASTM D792, Standard Test Methods for Density and Specific Gravity (Relative Density) of Plastics by Displacement, ASTM International, West Conshohocken, PA, 2013, www.astm.org
30. Y. Li, P. Xiao, Z. Li, W. Zhou, T. Liensdorf, W. Freudenberg, N. Langhof, and W. Krenkel, *Ceram. Int.* 42 (2016) 6850-6857.
31. Y. Li, P. Xiao, H. Luo, R.S.M. Almeida, Z. Li, W. Zhou, A. Bruckner, F. Reichert, N. Langhof, and W. Krenkel, *J. Eur. Ceram. Soc.* 36 (2016) 3977-3985.
32. Y. Li, P. Xiao, Y. Shi, R.S.M. Almeida, W. Zhou, Z. Li, H. Luo, F. Reichert, N. Langhof, and W. Krenkel, *Composites: Part A* 95 (2017) 315-324.
33. X. Wu, N. Langhof, W. Krenkel, R. Habath, and F. Lenz, *Ceram. Int.* 44 (2018) 16325-16332.
34. Z. Ma, *Ceram. Int.* 44 (2018) 13145-13151.
35. P. Sangsuwan, S.N. Tewari, J.E. Gatica, M. Singh, and R. Dickerson, *Metall Mater Trans B* 30 (1999) 933-944.